ACS NANO

Cite This: ACS Nano 2018, 12, 12247−12254

www.acsnano.org

ARTICLE

Combined Use of Unnatural Amino Acids Enables Dual-Color Super-Resolution Imaging of Proteins *via* Click Chemistry

Kim-A. Saal,*,† Frank Richter,‡ Peter Rehling,‡ and Silvio O. Rizzoli*,†

†Institute for Neuro- and Sensory Physiology, Center for Biostructural Imaging of Neurodegeneration, University Medical Center Göttingen, Cluster of Excellence Nanoscale Microscopy and Molecular Physiology of the Brain, Göttingen, Germany

‡Institute for Cellular Biochemistry, University Medical Center Göttingen, Göttingen, Germany

Supporting Information

ABSTRACT: **Recent advances in optical nanoscopy have brought the imaging resolution to the size of the individual macromolecules, thereby setting stringent requirements for the fluorescent labels. Such requirements are optimally fulfilled by the incorporation of unnatural amino acids (UAAs) in the proteins of interest (POIs), followed by fluorophore conjugation *via* click chemistry. However, this approach has been limited to single POIs in mammalian cells. Here we solve this problem by incorporating different UAAs in different POIs, which are expressed in independent cell sets. The cells are then fused, thereby combining the different proteins and organelles, and are easily imaged by dual-color super-resolution microscopy. This procedure, which we termed Fuse2Click, is simple, requires only the well-established Amber codon, and allows the use of all previously optimized UAAs and tRNA/RS pairs. This should render it a tool of choice for multicolor click-based imaging.**

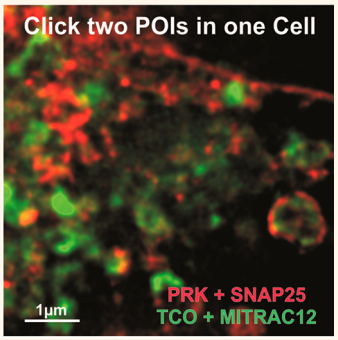

KEYWORDS: *unnatural amino acid, dual color, click chemistry, cycloaddition, super-resolution, STED, cell−cell fusion*

Super-resolution fluorescence microscopy has progressed strongly over the past decade, moving from resolutions of ∼60−70 nm in the first biological applications to ∼1 nm in some of the most recent developments.[1−3] This enabled the analysis of different cellular structures with much higher precision than was possible in the past, and a number of seminal discoveries have indeed been made, including the periodic organization of actin in thin cellular processes[4] or of molecules in the nuclear pore.[5]

Nevertheless, a number of limitations have also become obvious, especially concerning the precision with which the different molecules can be tagged fluorescently. The tags used should not displace the fluorophores from the proteins of interest (POIs), and they should not affect the localization and the function of the POIs. Several tags that have been classically used in conventional microscopy have difficulties in fulfilling these requirements. Conventional antibodies are large (∼15 nm in size) and thus place the fluorophores too far from the intended targets, especially if packages of primary and secondary antibodies are used.[5,6] Camelid-derived nanobodies alleviate this problem, in part, by their smaller size,[7] and their use as replacements for conventional secondary antibodies is promising.[8] However, only a few nanobodies are currently available, for a handful of POIs. Genetically encoded labels, such as the fluorescent proteins, are substantially smaller than antibodies[9] and can be coupled to a variety of targets without affecting their molecular or functional characteristics too drastically,[10] but are typically not as bright nor as photostable as the chemical fluorophores that are commonly conjugated to antibodies or nanobodies.

A nanoscopy tag that is substantially smaller than fluorescent proteins and enables the use of almost any desired fluorophore has been obtained by reprogramming the genetic code, which enables the encoding of unnatural amino acids (UAAs) into the POIs.[11,12] In brief, this entails the expression of orthogonal pairs of tRNAs and aminoacyl-tRNA synthetases (tRNA/RS), together with genes that code for the POIs, which contain at least one Amber stop codon (TAG). The tRNA/RS expressed in the cells recognize the Amber codon with high specificity and can incorporate an appropriately chosen UAA into the protein sequence during translation. The UAA carries a chemical functionality that enables its conjugation to the desired fluorophore. For example, the UAA propargyl-L-lysine (PRK) contains an alkyne group that can be conjugated to fluorophores carrying an azide functionality, through the so-called "click reaction" (copper-mediated azide−alkyne cycloaddition).[13,14] The fluorophores are typically attached to the molecules after fixation, although live cell coupling is also

Received: August 8, 2018
Accepted: December 10, 2018
Published: December 10, 2018

DOI: 10.1021/acsnano.8b06047
ACS Nano 2018, 12, 12247−12254

possible.[15] This ensures that the biological effects of the tag are as small as possible, since the POI suffers no interference from the fluorophore, until fixation. At the same time, the small tag size, of only one amino acid side chain, places the fluorophore in the immediate vicinity of the POI.

One major problem with this approach, however, has been the tagging of multiple POIs simultaneously. This is mainly due to the fact that only the Amber codon is relatively easy to use for the incorporation of UAAs, while other codons are far more difficult to employ. This issue has been easier to solve in *E. coli*, where optimization of the different elements of the UAA/click chemistry system has enabled the use of both the Amber and the Ochre (TAA) codons simultaneously.[16,17] This solution has also been attempted in mammalian cells, where two different UAAs could be introduced, at distinct sites, in the same POI.[18] However, the use of this system remains extremely difficult and is still under considerable optimization, before it may be available for labeling two different POIs.[19,20] Another solution has been to use quadruplet-decoding ribosomes, which no longer need to rely on stop codons.[21] Combining this approach with the Amber codon-based incorporation of UAAs enabled dual UAA use in *E. coli*.[22] Although the quadruplet-decoding approach is possible in mammalian cells,[23] its combination with other tools has been problematic, thus rendering the dual-color imaging of POIs extremely difficult in this system.[24]

One further possibility has been to label the same POI with two UAAs, by applying them sequentially.[15] This approach provides dual-color imaging, but still only reveals one POI, thus highlighting the need for true dual-color/dual-POI imaging.

We set out here to solve this problem by arguing that the Amber system has been thoroughly optimized in mammalian cells, and thus it would be desirable to use it for multiple POIs, without relying on other, less well optimized, systems (*e.g.*, Ochre or quadruplet systems). The fundamental difficulty in this approach is that the incorporation of the Amber codon in two POIs in the same cell would induce the incorporation of any UAAs in both proteins, without discrimination.

To solve this problem, we decided to express two different proteins in two separated sets of cells, which incorporate two different UAAs. The cells are then fused, which allows the proteins and organelles to intermix. After a certain time, cells are fixed, and fluorophores can be specifically coupled to the POIs *via* the applicable click reactions, thus enabling the investigation of the two different proteins in super-resolution microscopy. We termed this approach of applying dual-color click chemistry for two different POIs with the help of cell−cell fusion Fuse2Click.

RESULTS AND DISCUSSION

With the help of cell−cell fusion, we established a method to easily tag two different POIs simultaneously by click chemistry. We decided to express one Amber-containing POI in a first set of cells in the presence of the UAA propargyl-L-lysine together with pyrrolysine tRNA-synthetase/tRNA pair wild-type (tRNA/RS^{WT}) from *Methanosarcina mazei*.[13,25] The translation process in these cells incorporates the alkyne-containing PRK into the POI.[26] A second Amber-containing POI is simultaneously expressed in a second set of cells, which coexpress a pair of tRNA and the double mutant Y306A, Y384F of *M. mazei* pyrrolysyl-tRNA-synthetase (tRNA/RS^{AF}).[25] With the help of tRNA/RS^{AF} it is possible to incorporate the second UAA, *trans*-cyclooctene−L -lysine (TCO*A, in the following termed TCO),[15,24,27] into the second POI (Figure 1). The cells are allowed to express the proteins for the desired time period, and they are then induced to fuse using inactivated Sendai virus particles.[28,29] The cells fuse readily and intermix fully their plasma membranes within 30−60 min, as we have observed in the past.[29] The proteins, containing either PRK or TCO, are thus placed in each other's vicinity (Figure 1). After a suitable time period, chosen by the experimenter according to the desired biological effects, the cells are fixed and are subjected first to strain-promoted inverse-electron demand Diels−Alder cycloaddition (SPIEDAC) to label TCO with the help of a Star580-tetrazine.[30] Subsequently, PRK-containing proteins can be identified with

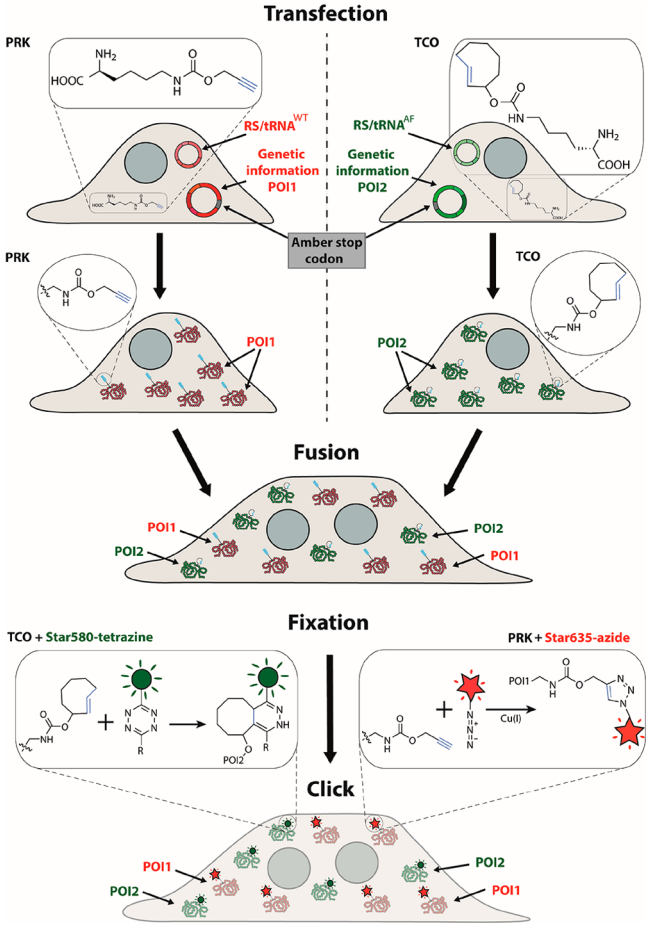

Figure 1. Parallel expression of Amber-containing POI genes in separate sets of cells, followed by cell−cell fusion, enables dual-color click chemistry (Fuse2Click). The scheme of the experimental design shows two separately transfected sets of cells. The first set receives PRK, together with the genetic information for protein of interest 1 (POI1), which contains an Amber stop codon, and a RS/tRNA^{WT} pair, which enables the incorporation of PRK. Simultaneously, TCO is added to the second set of cells, together with the plasmid for the protein of interest 2 (POI2), also containing an Amber codon, and a RS/tRNA^{AF} pair, for TCO incorporation. Both amino acids are incorporated in the respective cells. The two sets of cells are then pooled and are fused using inactivated Sendai virus envelope particles. After fusion the cells are subjected to click chemistry reactions, thereby coupling the two POIs specifically to different fluorophores, which can then be revealed by fluorescence microscopy.

DOI: 10.1021/acsnano.8b06047
ACS Nano 2018, 12, 12247−12254

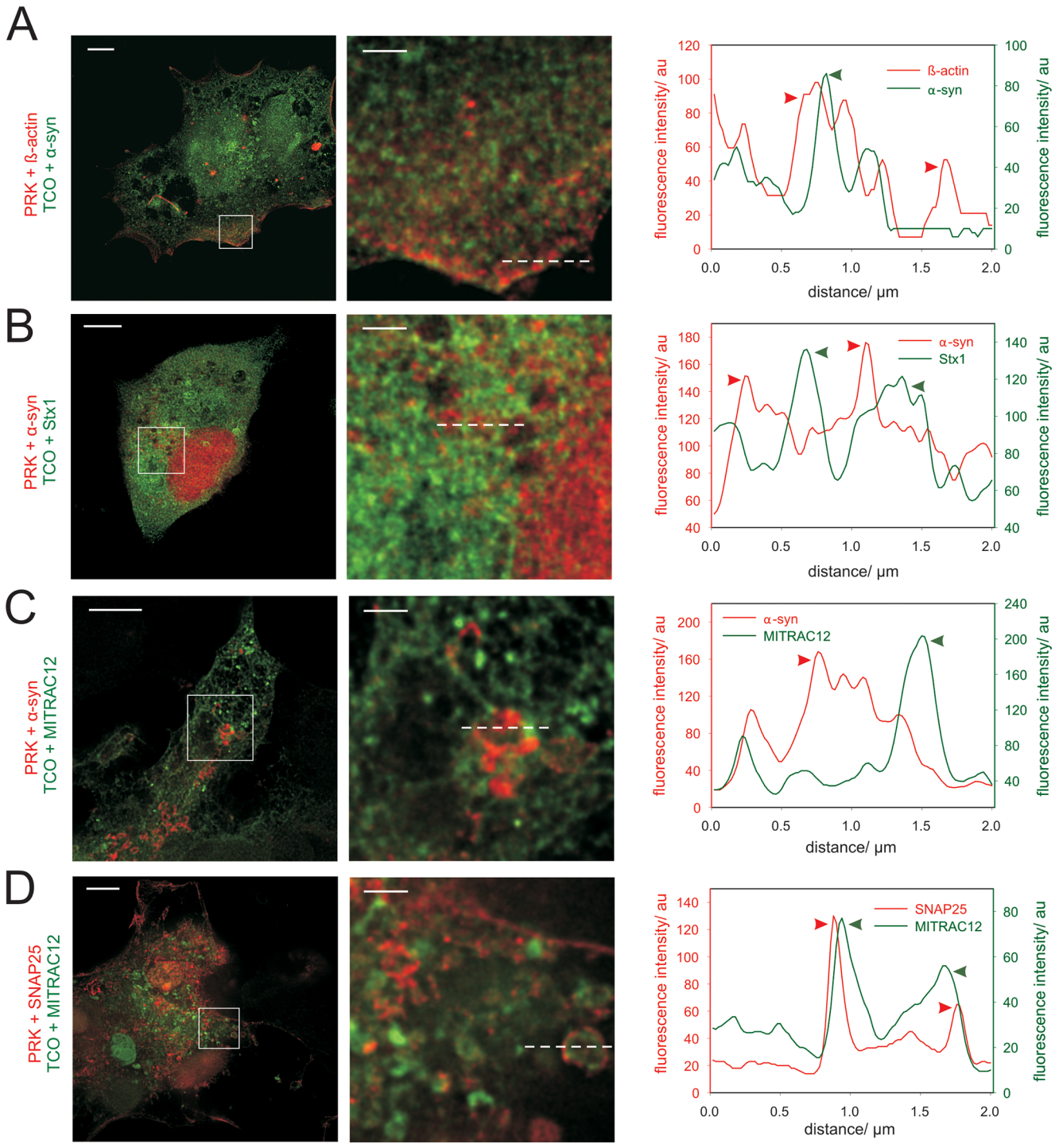

Figure 2. Two-color STED microscopy of fused cells expressing different pairs of Amber-containing POIs. (A) *β*-actin and *α*-synuclein (*α*-syn). The line scan indicated as a white dotted line in the right panel reveals that *α*-synuclein (green arrowhead) forms assemblies that intersperse with the actin cytoskeleton (red arrowhead) on the plasma membrane. (B) Syntaxin 1 (Stx1) and *α*-synuclein (*α*-syn). Overexpressed syntaxin 1 (green arrowhead) remains in the endoplasmic reticulum in these cells,[10] which does not appear to colocalize with the cytosol marked by *α*-synuclein (red arrowhead), as indicated by the line scan. (C) MITRAC12 and *α*-synuclein (*α*-syn). This experiment reveals that *α*-synuclein (red arrowhead) can indeed line the mitochondria assemblies (green arrowhead in the line scan), as discussed in the literature.[38,39] (D) SNAP25 and MITRAC12. The plasma membrane protein SNAP25, a neuronal protein, distributes itself to many cellular membranes upon overexpression in fibroblasts. Interestingly, in the shown example such membranes (red arrowheads) contact and line a mitochondrion (green arrowheads) as illustrated in the line scan. Scale bars: 5 *µ*m for overviews (left column) and 1 *µ*m for zoom panels (right column).

the addition of Star635P-azide *via* copper-catalyzed alkyne–azide cycloaddition (CuAAC).[15,31] This conjugates the desired fluorophores specifically on the two POIs and enables their identification in microscopy (Figure 2).

DOI: 10.1021/acsnano.8b06047
ACS Nano 2018, 12, 12247–12254

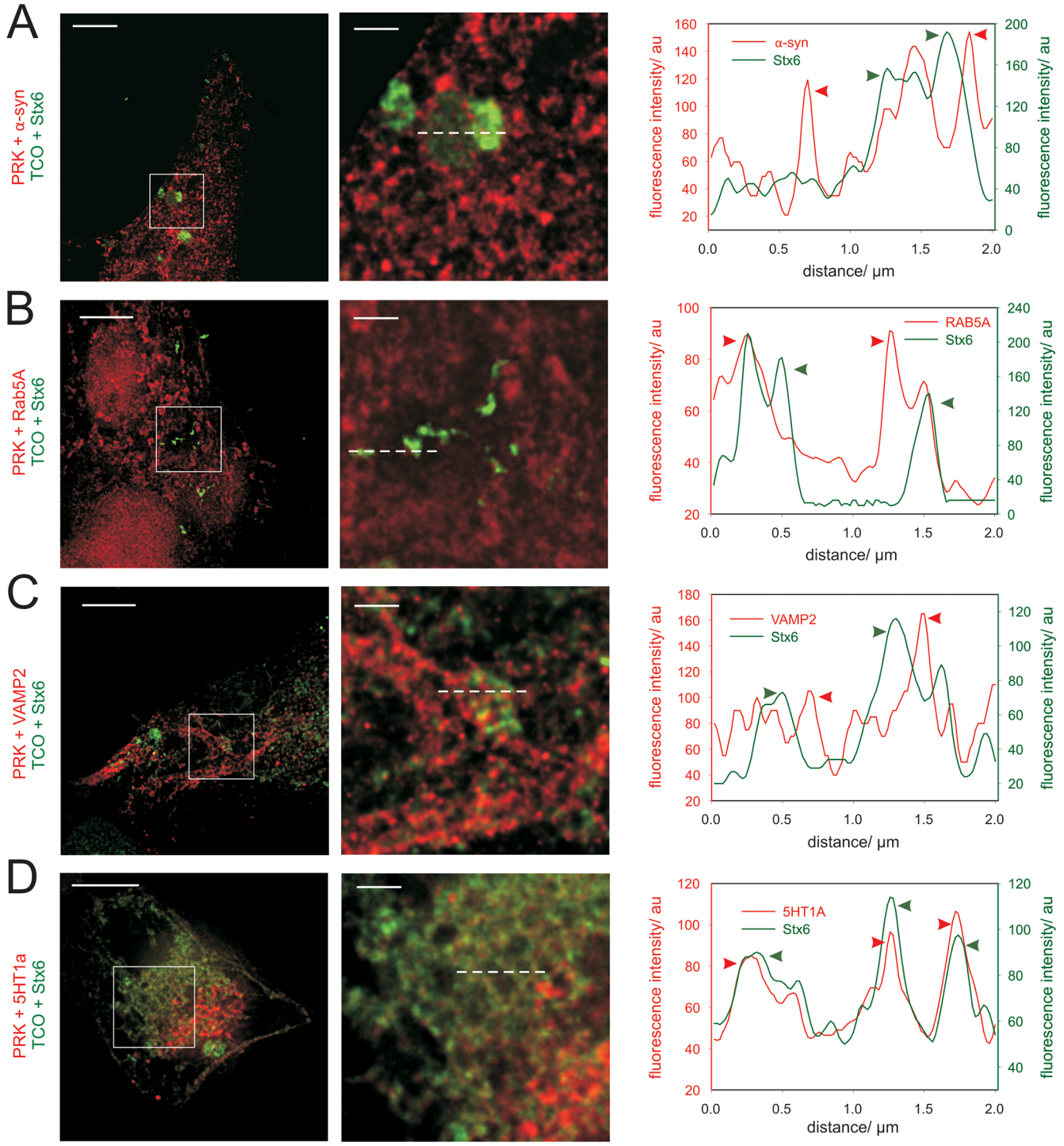

Figure 3. Further examples of two-color STED microscopy of fused cells expressing different pairs of Amber-containing POIs. In this figure we grouped examples showing different proteins colocalizing with the SNARE fusion protein syntaxin 6 (Stx6), which distributes to secretory organelles from the Golgi apparatus to sorting endosomes.[33] (A) Syntaxin 6 and α-synuclein (α-syn). The line scan (white dotted line in detail image) indicates that α-synuclein (red arrowhead) can line the membranes of the syntaxin 6-containing organelles (green arrowheads). (B) Syntaxin 6 and Rab5A. The sorting endosome marker Rab5A (red arrowheads) colocalizes with syntaxin 6-containing organelles (green arrowheads). (C) Syntaxin 6 and VAMP2. The neuronal SNARE VAMP2 (red arrowheads) is expressed in different cellular vesicles,[40] which overlap partially with the syntaxin 6-containing organelles (green arrowheads, see also ref 41) for antibody-based investigations of these proteins. (D) Syntaxin 6 and 5HT1a. The two molecules colocalize (Stx6: green arrowheads, 5HT1A: red arrowheads) extensively in the endosome system of the fused cells (line scan). Scale bars: 5 μm overview (left column); 1 μm detail.

Both PRK and TCO were incorporated into the POIs selectively, and no signals were observed when the POIs were not expressed (Supplementary Figure S1). The proteins could then be conjugated to fluorophores in a highly specific fashion, with negligible background (Supplementary Figure S1). To place the different POIs together, we applied the cell fusion procedure (Figures 2 and 3). For two-color imaging we conjugated TCO to the fluorophore Abberior Star580

DOI: 10.1021/acsnano.8b06047
ACS Nano 2018, 12, 12247−12254

(represented in green in all figures), and we conjugated PRK to Abberior Star635P (red in all figures). Only fused cells showed both green and red fluorescence. No dual-color cells were observed when the cells were only cultured together, but were not induced to fuse (Supplementary Figure S2). The two fluorophores allowed for efficient two-color stimulated emission depletion (STED) imaging, with a resolution of ~40 nm (Supplementary Figure S3). The complete intermixing of the cell components after cell fusion required ~60 min to intermix (Supplementary Figure S4). Substantially longer incubation times after fusion (>2 h) might lead to cross-incorporation of the UAAs into both POIs. After fusion both UAAs are present in the fused cells, along with both RS/tRNA pairs, which can now blindly incorporate the UAAs at the Amber codons of the two POIs. Examples and a detailed analysis are shown in Supplementary Figure S5.

We first tested Fuse2Click by choosing as POIs the cytoskeletal component actin and α-synuclein, a soluble protein that has the capacity to form aggregates that may interact with different cellular membranes. Both proteins are organized as expected (Figure 2A). Actin forms cytoskeletal arrangements especially in the vicinity of the plasma membrane of the fused cell, and α-synuclein forms various arrangements both in the nuclei and in the cytosol (see for comparison STED images of α-synuclein).[32] We have also tested the neuronal plasma membrane SNARE fusion proteins syntaxin 1 and SNAP25,[33] the mitochondria marker MITRAC12 (COA3),[34] the vesicular SNARE f protein VAMP2/synaptobrevin 2,[33] the Golgi apparatus- and endosome-located SNARE protein syntaxin 6,[33] the endosomal marker Rab 5 (a membrane-organizing protein of the endosome),[35] and the serotonin receptor 5HT1a.[36] While a discussion of the different protein distributions is beyond the scope of this article, the different experiments suggest the following. First, the proteins remain targeted to the appropriate compartments. For example, MITRAC12 is an integral inner membrane protein that does not leave the mitochondrion (Figure 2C,D), and the cytosolic α-synuclein does not penetrate into the organelles labeled by syntaxin 6 (Figure 3A). Second, expected protein−organelle contacts are indeed observed, as in the case of α-synuclein lining the organelles defined by syntaxin 6 (Figure 3A) and MITRAC12 (Figure 2C) or of Rab5 on organelles of the secretory pathway defined by syntaxin 6 (Figure 3B). Third, the cell fusion not only enables organelles and various proteins to intermix (all panels of Figures 2 and 3) but is also sufficient to enable the molecules that are targeted to the same organelles to intermix, presumably by organelle fusion. This is clear in the case of syntaxin 6 and 5HT1a (Figure 3D). Moreover, several organelle contacts are also evident, as in the case of the tight contacts between SNAP25-labeled membranes and mitochondria (Figure 2D) or between the VAMP2- and syntaxin 6-defined organelles (Figure 3C). This implies that the cell fusion assay is sufficiently robust to reveal a large number of molecule and organelle interactions in the cells.

As a note of caution, we would like to point out that since these experiments rely on overexpression of different proteins, the experimenter should carefully select the fused cells, only imaging the ones that appear physically intact and do not show signs of overexpression-induced cell death. We suggest avoiding cells with very high fluorescence levels, with a rounded cell shape and/or membrane bulges and bursts or with numerous large vacuoles. Fortunately, this problem, which is common to any experiments using overexpression, is not very serious for Fuse2Click. Dead cells cannot fuse to other cells, and sick cells also typically do not fuse (one example is shown in Supplementary Figure S6, found after surveying hundreds of normal-looking fused cells).

CONCLUSION

We conclude that Fuse2Click is a readily feasible solution to the problem of labeling multiple POIs *via* click chemistry, which can be applied to a multitude of targets. To enable its easy reproduction in other laboratories, we present a complete protocol in the supplementary methods, a time line of the fusion reaction (Supplementary Figure S7), which should enable investigators to choose the optimal time period after fusion that is required in their specific experiments and some potential pitfalls of the click reactions (Supplementary Figure S8).

Fuse2Click still has several shortcomings from a biological point of view. For example, the interaction between nuclear POIs is difficult to study by this approach, since the nuclei are not expected to fuse and to thus place their POIs together on a rapid time scale. Soluble nuclear POIs may be exchanged between the nuclei, as probably does α-synuclein in Figure 2A (this molecule has labeled both nuclei of the two fused cells in the particular image). However, this would not be an option for molecules that cannot leave the nuclei (for example histones or nuclear pore proteins), and hence such proteins cannot be studied *via* Fuse2Click. Other organelles and proteins are much more dynamic, as shown in Figures 2 and 3, but some degree of optimization will be needed for every organelle or protein system, to ensure that sufficient time is allowed after cellular fusion, for the perfect intermixing of the respective targets.

At the same time, this approach holds several important advantages. It is readily performed (Supplementary Figure S7), and any combination of UAAs and tRNA/RS systems can be used, as long as they allow the conjugation of the fluorophores by two different reactions. We believe that this system will be most useful for the investigation of organelle contact sites, since these elements require both high resolution and high labeling densities and are therefore difficult to study using conventional methods as antibody-based immunostainings. The system is not, in principle, limited to two POIs and two colors. The cellular fusion process is efficient and can accommodate multiple cell sets (at least four, in our own experiments). This would extend the analysis to even more UAA combinations, with the caveat that the labeled POIs would become diluted in the larger cell volume generated by the fusion of multiple cells. This caveat, however, has already been addressed by the development of highly efficient click reactions,[37] which should ensure optimal labeling, which should still be more intense than that obtainable with antibody-based immunostainings, due to the latter's poorer epitope-revealing efficiency.[9]

MATERIALS AND METHODS

In the Supporting Information a full description of materials, as well as a detailed protocol for the practical implementation of Fuse2Click is included.

Cells. In this study baby hamster kidney (BHK) fibroblasts were used and cultured in Dulbecco's modified Eagle's medium (DMEM), supplemented with 10% tryptose phosphate, 5% fetal bovine serum (FBS), 2 mM L-glutamine, 60 U/mL penicillin, and 60 U/mL

DOI: 10.1021/acsnano.8b06047
ACS Nano 2018, 12, 12247−12254

streptomycin. Cells were passaged every 3−4 days and used for experiments up to 25 passages.

Constructs. Amber stop containing DNA constructs were produced in-house as previously described in Vreja *et al.*, 2015.[26] As an additional protein the mitochondrial POI MITRAC12 was chosen. Here, the point mutation A37T was introduced into the sequence of C-terminally tagged MITRAC12FLAG in pcDNA5, leading to the Amber stop codon TAG instead of lysine at position 13 (MITRAC12FLAGK13TAG). For this purpose, the following partially overlapping primers, with the desired mutation, were designed: Fwd: 5′-ctggattcttagcgtggagaggccccgttcgc-3′; Rev: 5′-gcctctccacgctaagaatccagagggtcacc-3′. This was done according to Zheng and co-workers (2004).[42] PCR was performed using the KOD Hot Start DNA polymerase kit (Novagen), and the instructions given by the manufacturer were followed. MITRAC12FLAG in pcDNA5 was used as a template, and PCR conditions were 95 °C (3′), followed by 20 cycles of 95 °C (20″), 60 °C (10″), and 70 °C (3′). The reaction was cooled to 4 °C, and the enzyme Dpn1 (Thermo Scientific) was added at 37 °C (60′) to digest parental DNA. Digested plasmid was used for transformation and subsequent plasmid isolation and sequencing. The vectors pCMV tRNA/RSWT and pCMV tRNA/RSAF were provided from Lemke laboratory and applied as earlier depicted.[15,27]

Incorporation of UAA into Proteins of Interest. Two sets of BHK cells were grown in culture medium without antibiotic supplements. One set of cells was seeded on 18 mm glass coverslips (CS; ∼20 000 cells/CS), while the other set were grown in a six-well multiwell plate (∼60 000 cells/well). Twenty four hours after seeding, transfection was performed by adding the DNA encoding for the protein of interest containing the Amber stop codon for POI1 together with the vector encoding for tRNA/RS^{WT} into Opti-MEM (Gibco). The vector encoding for POI2 was mixed together with the vector for tRNA/RS^{AF} into another tube containing Opti-MEM. Lipofectamine 2000 reagent (Life Technologies) was separately equilibrated in Opti-MEM for 5 min. Afterward Lipofectamine/Opti-MEM was added to both DNA mixtures and incubated for 20 min at room temperature (RT). In the meanwhile, 250 μM PRK was added to the set of cells that are attached to CS, while 400 μM TCO was added to the set of cells that were grown in a six-well multiwell plate. Subsequently, the vector/Lipofectamine mixtures were added to the respective cell sets (vector POI1 + tRNA/RS^{WT} to PRK-treated cells on CS; vector POI2 + tRNA/RS^{AF} to TCO-treated cells in a six-well multiwell plate). Cells were incubated at 37 °C and 5% CO_2 for 18−24 h to incorporate UAA and express the proteins (refer to Figure S7: experimental timeline). Afterward medium was exchanged with normal DMEM BHK culture medium.

Cell−Cell Fusion. Having now two sets of cells expressing two different POIs, with either incorporated PRK or TCO, respectively, cell−cell fusion was performed: Cells that incorporated TCO were detached from a six-well multiwell plate, collected, and treated with inactivated Sendai virus particles (Sendai virus envelope, HVJ-E, provided as HVJ envelope cell fusion kit GenomONE-CF Ex, Cosmo Bio) according to the manufacturer's instructions. Afterward, these cells were added on top of the other cell set (which incorporated PRK) on CS and were centrifuged in plate to force fusion of cells. Sixty minutes after initiation of fusion cells were fixed with 4% paraformaldehyde (PFA) in phosphate-buffered saline (PBS).

Click reaction. PFA-fixed cells were quenched in 100 mM NH_4Cl in PBS for 20 min at RT, followed by permeabilization with 0.1% Triton-X 100 in PBS and blocking with a mixture of 5% bovine serum albumin (BSA) and 5% tryptone/peptone (Carl Roth GmbH) in 0.1% Triton-X 100 in PBS. Directly before starting the click reactions, cells were rinsed with 3% BSA in PBS. First, the SPIEDAC was performed to label TCO in POI2 with Star580, by incubating the CS in 3% BSA in PBS containing 0.2 μM Star580-tetrazine for 10 min in a humidified chamber protected from light. Second, cells were washed 5 min with PBS before being subjected to the CuAAC to click PRK with Star635P. For this purpose the Click-iT cell reaction buffer kit (Life Technologies) was applied according to the manufacturer's instructions. In brief, a mixture of Click-iT reaction buffer (component A), 2 mM $CuSO_4$ (component B), Click-iT reaction buffer additive (component C), and 20 μM Star635P-azide was prepared in H_2O, and CS was immediately incubated in this reaction mixture protected from light in a humidified chamber for 30 min.

Hoechst Staining and Embedding. After the click reaction, cells were washed 15 min with 5% tryptone/peptone in PBS, followed by 5 min of incubation in 2 μM Hoechst to label cell nuclei. Before embedded in Mowiol 4-88 mounting medium (Carl Roth GmbH), cells were extensively washed with PBS.

Confocal and STED Microscopy. Confocal and STED images were generated by employing a multicolor microscope setup (Abberior Instruments) based on an IX83 microscope (Olympus) equipped with an UPLSAPO 100× 1.4 NA oil immersion objective (Olympus). To obtain confocal images of Star635P, a 640 nm excitation laser (set to 5−15% of max. power of 1.77 mW) was employed, and signal was detected with an avalanche photodiode unit (APD) in a range between 650 and 720 nm. Star580 was visualized with a 561 nm excitation laser (set to 40% of max. power of 440 μW), and the emission signal was detected with an APD in a range between 605 and 625 nm. For STED imaging excitation of Star fluorophores was obtained using a 640 nm laser for Star635P and a 580 nm laser for Star580, respectively, both pulsed with 80 MHz. Depletion for both fluorophores was effected by a 775 nm depletion laser (set to 40% of max. power of 1.2 W). Scanning was performed with a dwell time of 15 μs per pixel with a 20 nm pixel size. The images presented in Figure 2 and Figure 3 were processed by deconvolution, performed with Huygens Essential 4.4 (Scientific Volume Imaging, Hilversum, The Netherlands), relying on in-built algorithms.

Line Scans. The 2 μm long line scans, which are generated in the detailed images of Figures 2 and 3 (illustrated as a white dotted line), indicate the size and the orientation of representative pools of the particular POIs after cell−cell fusion, thereby giving information about the POIs' relationship of interaction (Figures 2 and 3). The line scans were performed in Matlab (The Mathworks, Inc., Natick, MA, USA), under direct command of the user.

To illustrate the STED effect, we performed 500 nm long line scans (red and green framed lines) through a representative structure of two POIs in confocal generated images, as well as through exactly the same structure obtained by STED scan (Supplementary Figure S3), in the same fashion as for Figures 2 and 3.

ASSOCIATED CONTENT

Supporting Information

The Supporting Information is available free of charge on the ACS Publications website at DOI: 10.1021/acsnano.8b06047.

Reagents and materials, epifluorescence microscopy, Figures S1, S2, S3, S4, S5, S6, S7, and S8, and a detailed protocol for practical application of Fuse2Click (PDF)

Source data (PDF)

AUTHOR INFORMATION

Corresponding Authors

*E-mail: kim-ann.saal@med.uni-goettingen.de.
*E-mail: srizzol@gwdg.de

ORCID

Silvio O. Rizzoli: 0000-0002-1667-7839

Author Contributions

K.-A.S. performed all of the experiments. F.R. and P.R. contributed the MITRAC12 Amber stop construct. S.O.R. conceived the project and performed the line scans. S.O.R. and K.-A.S. wrote the manuscript.

Notes

The authors declare no competing financial interest.

DOI: 10.1021/acsnano.8b06047
ACS Nano 2018, 12, 12247−12254

ACKNOWLEDGMENTS

We thank I. Vreja for her preliminary work on building the Amber-containing vectors and for her help in the beginning of this study. This work was supported by grants to S.O.R. from the European Research Council (ERC-2013-CoG Neuro-MolAnatomy) and from the Deutsche Forschungsgemeinschaft (DFG): 1967/7-1 and SFB1190/P09. The work on MITRAC12 was supported by the Boehringer Ingelheim Fonds (FR), the Ph.D. program "Molecular Biology"–International Max Planck Research School, and the Göttingen Graduate School for Neurosciences and Molecular Biosciences (GGNB; DFG grant GSC 226/1) (F.R.) and by grants to P.R. from ERCAdG 339580 MITRAC and SFB1286/A6.

REFERENCES

(1) Sahl, S. J.; Hell, S. W.; Jakobs, S. Fluorescence Nanoscopy in Cell Biology. *Nat. Rev. Mol. Cell Biol.* **2017**, *18*, 685–701.
(2) Willig, K. I.; Rizzoli, S. O.; Westphal, V.; Jahn, R.; Hell, S. W. STED Microscopy Reveals That Synaptotagmin Remains Clustered after Synaptic Vesicle Exocytosis. *Nature* **2006**, *440*, 935–939.
(3) Balzarotti, F.; Eilers, Y.; Gwosch, K. C.; Gynnå, A. H.; Westphal, V.; Stefani, F. D.; Elf, J.; Hell, S. W. Nanometer Resolution Imaging and Tracking of Fluorescent Molecules with Minimal Photon Fluxes. *Science* **2017**, *355*, 606–612.
(4) Xu, K.; Zhong, G.; Zhuang, X. Actin, Spectrin, and Associated Proteins Form a Periodic Cytoskeletal Structure in Axons. *Science* **2013**, *339*, 452–456.
(5) Szymborska, A.; de Marco, A.; Daigle, N.; Cordes, V. C.; Briggs, J. A. G.; Ellenberg, J. Nuclear Pore Scaffold Structure Analyzed by Super-Resolution Microscopy and Particle Averaging. *Science* **2013**, *341*, 655–658.
(6) Opazo, F.; Levy, M.; Byrom, M.; Schäfer, C.; Geisler, C.; Groemer, T. W.; Ellington, A. D.; Rizzoli, S. O. Aptamers as Potential Tools for Super-Resolution Microscopy. *Nat. Methods* **2012**, *9*, 938–939.
(7) Ries, J.; Kaplan, C.; Platonova, E.; Eghlidi, H.; Ewers, H. A Simple, Versatile Method for GFP-Based Super-Resolution Microscopy *via* Nanobodies. *Nat. Methods* **2012**, *9*, 582–584.
(8) Pleiner, T.; Bates, M.; Görlich, D. A Toolbox of Anti – Mouse and Anti – Rabbit IgG Secondary Nanobodies. *J. Cell Biol.* **2018**, *217*, 1143–1154.
(9) Maidorn, M.; Rizzoli, S. O.; Opazo, F. Tools and Limitations to Study the Molecular Composition of Synapses by Fluorescence Microscopy. *Biochem. J.* **2016**, *473*, 3385–3399.
(10) Vreja, I. C.; Kabatas, S.; Saka, S. K.; Kröhnert, K.; Höschen, C.; Opazo, F.; Diederichsen, U.; Rizzoli, S. O. Secondary-Ion Mass Spectrometry of Genetically Encoded Targets. *Angew. Chem., Int. Ed.* **2015**, *54*, 5784–5788.
(11) Chin, J. W. Expanding and Reprogramming the Genetic Code. *Nature* **2017**, *550*, 53–60.
(12) Young, T. S.; Schultz, P. G. Beyond the Canonical 20 Amino Acids: Expanding the Genetic Lexicon. *J. Biol. Chem.* **2010**, *285*, 11039–11044.
(13) Milles, S.; Tyagi, S.; Banterle, N.; Koehler, C.; Vandelinder, V.; Plass, T.; Neal, A. P.; Lemke, E. a. Click Strategies for Single Molecule Protein Fluorescence. *J. Am. Chem. Soc.* **2012**, *134*, 5187–5195.
(14) Kolb, H. C.; Finn, M. G.; Sharpless, K. B. Click Chemistry: Diverse Chemical Funtion from a Few Good Reactions. *Angew. Chem., Int. Ed.* **2001**, *40*, 2004–2021.
(15) Nikić, I.; Plass, T.; Schraidt, O.; Szymański, J.; Briggs, J. A. G.; Schultz, C.; Lemke, E. A. Minimal Tags for Rapid Dual-Color Live-Cell Labeling and Super-Resolution Microscopy. *Angew. Chem., Int. Ed.* **2014**, *53*, 2245–2249.
(16) Wan, W.; Huang, Y.; Wang, Z.; Russell, W. K.; Pai, P. J.; Russell, D. H.; Liu, W. R. A Facile System for Genetic Incorporation of Two Different Noncanonical Amino Acids into One Protein in Escherichia Coli. *Angew. Chem., Int. Ed.* **2010**, *49*, 3211–3214.
(17) Chatterjee, A.; Sun, S. B.; Furman, J. L.; Xiao, H.; Schultz, P. G. A Versatile Platform for Single- and Multiple-Unnatural Amino Acid Mutagenesis in Escherichia Coli. *Biochemistry* **2013**, *52*, 1828–1837.
(18) Xiao, H.; Chatterjee, A.; Choi, S.; Bajjuri, K. M.; Sinha, S. C.; Schultz, P. G. Genetic Incorporation of Multiple Unnatural Amino Acids into Proteins in Mammalian Cells. *Angew. Chem., Int. Ed.* **2013**, *52*, 14080–14083.
(19) Zheng, Y.; Mukherjee, R.; Chin, M. A.; Igo, P.; Gilgenast, M. J.; Chatterjee, A. Expanding the Scope of Single- and Double-Noncanonical Amino Acid Mutagenesis in Mammalian Cells Using Orthogonal Polyspecific Leucyl-TRNA Synthetases. *Biochemistry* **2018**, *57*, 441–445.
(20) Zheng, Y.; Addy, P. S.; Mukherjee, R.; Chatterjee, A. Defining the Current Scope and Limitations of Dual Noncanonical Amino Acid Mutagenesis in Mammalian Cells. *Chem. Sci.* **2017**, *8*, 7211–7217.
(21) Neumann, H.; Wang, K.; Davis, L.; Garcia-Alai, M.; Chin, J. W. Encoding Multiple Unnatural Amino Acids *via* Evolution of a Quadruplet-Decoding Ribosome. *Nature* **2010**, *464*, 441–444.
(22) Wang, K.; Sachdeva, A.; Cox, D. J.; Wilf, N. W.; Lang, K.; Wallace, S.; Mehl, R. A.; Chin, J. W. Optimized Orthogonal Translation of Unnatural Amino Acids Enables Spontaneous Protein Double-Labelling and FRET. *Nat. Chem.* **2014**, *6*, 393–403.
(23) Niu, W.; Schultz, P. G.; Guo, J. An Expanded Genetic Code in Mammalian Cells with a Functional Quadruplet Codon. *ACS Chem. Biol.* **2013**, *8*, 1640–1645.
(24) Nikić, I.; Lemke, E. A. Genetic Code Expansion Enabled Site-Specific Dual-Color Protein Labeling: Superresolution Microscopy and Beyond. *Curr. Opin. Chem. Biol.* **2015**, *28*, 164–173.
(25) Plass, T.; Milles, S.; Koehler, C.; Schultz, C.; Lemke, E. A. Genetically Encoded Copper-Free Click Chemistry. *Angew. Chem., Int. Ed.* **2011**, *50*, 3878–3881.
(26) Vreja, I. C.; Nikić, I.; Göttfert, F.; Bates, M.; Kröhnert, K.; Outeiro, T. F.; Hell, S. W.; Lemke, E. A.; Rizzoli, S. O. Super-Resolution Microscopy of Clickable Amino Acids Reveals the Effects of Fluorescent Protein Tagging on Protein Assemblies. *ACS Nano* **2015**, *9*, 11034–11041.
(27) Plass, T.; Milles, S.; Koehler, C.; Szymański, J.; Mueller, R.; Wießler, M.; Schultz, C.; Lemke, E. A. Amino Acids for Diels-Alder Reactions in Living Cells. *Angew. Chem., Int. Ed.* **2012**, *51*, 4166–4170.
(28) Riento, K.; Frick, M.; Schafer, I.; Nichols, B. J. Endocytosis of Flotillin-1 and Flotillin-2 Is Regulated by Fyn Kinase. *J. Cell Sci.* **2009**, *122*, 912–918.
(29) Saka, S. K.; Honigmann, A.; Eggeling, C.; Hell, S. W.; Lang, T.; Rizzoli, S. O. Multi-Protein Assemblies Underlie the Mesoscale Organization of the Plasma Membrane. *Nat. Commun.* **2014**, *5*, 1–14.
(30) Blackman, M. L.; Royzen, M.; Fox, J. M. Tetrazine Ligation: Fast Bioconjugation Based on Inverse-Electron-Demand Diels-Alder Reactivity. *J. Am. Chem. Soc.* **2008**, *130*, 13518–13519.
(31) Lang, K.; Chin, J. W. Bioorthogonal Reactions for Labeling Proteins. *ACS Chem. Biol.* **2014**, *9*, 16–20.
(32) Lázaro, D. F.; Rodrigues, E. F.; Langohr, R.; Shahpasandzadeh, H.; Ribeiro, T.; Guerreiro, P.; Gerhardt, E.; Kröhnert, K.; Klucken, J.; Pereira, M. D.; Popova, B.; Kruse, N.; Mollenhauer, B.; Rizzoli, S. O.; Braus, G. H.; Danzer, K. M.; Outeiro, T. F. Systematic Comparison of the Effects of Alpha-Synuclein Mutations on Its Oligomerization and Aggregation. *PLoS Genet.* **2014**, *10*, 1004741–1004741.
(33) Jahn, R.; Scheller, R. H. SNAREs - Engines for Membrane Fusion. *Nat. Rev. Mol. Cell Biol.* **2006**, *7*, 631–643.
(34) Mick, D. U.; Dennerlein, S.; Wiese, H.; Reinhold, R.; Pacheu-Grau, D.; Lorenzi, I.; Sasarman, F.; Weraarpachai, W.; Shoubridge, E. A.; Warscheid, B.; Rehling, P. MITRAC Links Mitochondrial Protein Translocation to Respiratory-Chain Assembly and Translational Regulation. *Cell* **2012**, *151*, 1528–1541.
(35) Kiral, F. R.; Kohrs, F. E.; Jin, E. J.; Hiesinger, P. R. Rab GTPases and Membrane Trafficking in Neurodegeneration. *Curr. Biol.* **2018**, *28*, R471–R486.
(36) Niebert, S.; van Belle, G. J.; Vogelgesang, S.; Manzke, T.; Niebert, M. The Serotonin Receptor Subtype 5b Specifically Interacts

DOI: 10.1021/acsnano.8b06047
ACS Nano 2018, 12, 12247–12254

with Serotonin Receptor Subtype 1A. *Front. Mol. Neurosci.* **2017**, *10*, 1−14.
(37) Sachdeva, A.; Wang, K.; Elliott, T.; Chin, J. W. Concerted, Rapid, Quantitative, and Site-Specific Dual Labeling of Proteins. *J. Am. Chem. Soc.* **2014**, *136*, 7785−7788.
(38) Shavali, S.; Brown-Borg, H. M.; Ebadi, M.; Porter, J. Mitochondrial Localization of Alpha-Synuclein Protein in Alpha-Synuclein Overexpressing Cells. *Neurosci. Lett.* **2008**, *439*, 125−128.
(39) Guardia-Laguarta, C.; Area-Gomez, E.; Rub, C.; Liu, Y.; Magrane, J.; Becker, D.; Voos, W.; Schon, E. A.; Przedborski, S. α-Synuclein Is Localized to Mitochondria-Associated ER Membranes. *J. Neurosci.* **2014**, *34*, 249−259.
(40) Rizzoli, S. O. Synaptic Vesicle Recycling: Steps and Principles. *EMBO J.* **2014**, *33*, 788−822.
(41) Bethani, I.; Lang, T.; Geumann, U.; Sieber, J. J.; Jahn, R.; Rizzoli, S. O. The Specificity of SNARE Pairing in Biological Membranes Is Mediated by Both Proof-Reading and Spatial Segregation. *EMBO J.* **2007**, *26*, 3981−3992.
(42) Zheng, L.; Baumann, U.; Reymond, J.-L. An Efficient One-Step Site-Directed and Site-Saturation Mutagenesis Protocol. *Nucleic Acids Res.* **2004**, *32*, No. e115.

DOI: 10.1021/acsnano.8b06047
ACS Nano 2018, 12, 12247−12254